CHEMIJA
2026. Vol. 37. No. 1. P. 63–71

ISSN 0235-7216 eISSN 2424-4538
DOI: https://doi.org/10.6001/chemija.2026.37.1.7

Synthesis and properties of dimethoxytriphenylamine-based enamines

Jūratė Simokaitienė*,

Victor Lauroba Manrique,

Simas Mačionis,

Dmytro Volyniuk,

Eigirdas Skuodis,

Jonas Keruckas,

Juozas V. Gražulevičius

Department of Polymer Chemistry and Technology,
Faculty of Chemical Technology,
Kaunas University of Technology,
59 Baršausko Street,
51423 Kaunas, Lithuania

This article describes the synthesis and properties of new methoxy-substituted triphenylamine-based enamines. Thermal, photophysical and electrochemical properties of the compounds are reported. In addition, the ionisation energies estimated by photoelectron emission spectroscopy and hole transporting properties examined by the time-of-flight method are discussed. The compounds form molecular glasses with glass transition temperatures of up to 91°C. They exhibit a high thermal stability with 5% weight-loss temperatures above 420°C. Their characteristic optical band-gaps are of 2.9 eV and the solid-state ionisation energies situate around 5.4 eV. One of the compounds shows a high hole mobility of 8.4×10^{-4} cm^2/Vs at the electric field of 4×10^5 V/cm.

Keywords: enamines, 4,4′-dimethoxytriphenylamine, methoxy substituents, hole-transporting properties

INTRODUCTION

Nowadays, renewable energy sources such as photovoltaic devices and perovskite solar cells in particular represent one of the most active fields of research. One of the most important parts of perovskite solar cells are the hole-transporting layers which highly impact the efficiency of the devices. Suitable hole mobility, ionisation energy and electron affinity values as well as electrochemical stability of the hole-transporting compounds and morphological stability of their layers are important characteristics of materials used for the preparation of hole transporting layers [1]. Enamines are known to be efficient hole-transporting materials (HTMs) while methoxy-substitution is often utilised for the improvement of their performance in devices [2–4]. The attachment of methoxy groups can allow one to improve hole-transporting properties [5] and to reduce ionisation energy [6]. Triphenylamine derivatives are known for their excellent hole-transporting properties. They are widely used as HTMs in perovskite solar cells [7]. One of the best-known materials, spiro-OMeTAD, exhibits a good performance in perovskite solar cells; however, the hole mobility in its layers is relatively low (≈10^{-4} cm^2/Vs) [8].

Here, we report on the synthesis and properties of two new 4,4′-dimethoxytriphenylamine-based enamines. They were obtained by condensation of an appropriate secondary amine with 2,2-diphenylacetaldehyde or 2,2-bis(4-metoxyphenyl)acetaldehyde. The results of the study of the properties of the compounds demonstrate that the synthesised compounds exhibit a high thermal stability as well as favourable electrochemical, photophysical and

* Corresponding author. Email: jurate.simokaitiene@ktu.lt

charge-transporting properties. The synthesised compounds are characterised by ionization energies of 5.4 eV. Their 5% weight loss temperatures exceed 420°C. They are capable of the formation of molecular glasses with glass transition temperatures up to 91°C. In addition, they exhibit high hole mobilities of 3.6×10^{-4} and of 8.4×10^{-4} cm^2/Vs at the electric field of 4×10^5 V/cm.

EXPERIMENTAL

Methods and materials

The chemicals were purchased from *Sigma-Aldrich* and used as received without further purification. The reactions were monitored by thin-layer chromatography on ALUGRAM SIL G/UV254 plates and developed with UV light. ^1H and ^{13}C NMR spectra were recorded with a Bruker Avance III (400 MHz) spectrometer at ambient temperature. The chemical shifts (δ) are given in ppm relative to tetramethylsilane (TMS, δ = 0 ppm). Mass spectra (MS) were recorded with a Waters SQ Detector 2 mass spectrometer. A PerkinElmer Spectrum GX II FT-IR System was employed to record the infrared (IR) spectra. Thermogravimetric analysis (TGA) was conducted with a TGA Q50 equipment under 20°C/min heating rate under nitrogen atmosphere. Differential scanning calorimetry (DSC) measurements were performed with a DSC Q2000 apparatus in aluminium hermetic pans with a heating rate of 10°C/min. An electrothermal melting point apparatus MEL-TEMP 1302D was used to measure melting points via the capillary method. UV–vis absorption spectra of the dilute tetrahydrofuran (THF) solutions and thin solid layers of the compounds were recorded with an Avantes AvaSpec-2048XL equipment. Photoluminescence spectra of the dilute THF solutions and solid layers were recorded with an Edinburgh Instruments FLS980 system. Ionization potentials were measured by photoelectron emission spectroscopy using an ASBN-D130-CM deuter lamp as a UV source with a cm 110 1/8m monochromator and a Keithley 6517B electrometer.

Cyclic voltammetry measurements were carried out with a μAUTOLAB Type III potentiostat-galvanostat using a three electrode-system of 1 mm^2 Ag/Ag^+ working, Ag reference and Pt counter electrodes. The voltammograms were recorded of dichloromethane solutions with 0.1 M of tetrabutylamonium hexafluorophosphate as a supporting electrolyte.

The charge transporting properties of the compounds studied time of flight (TOF) techniques an EKSPLA NL300 laser (excitation wavelength of 355 nm), a 6517B electrometer (Keithley), a function generator AFG3011C (Tektronix) and a TDS 3032C oscilloscope (Tektronix) were used.

N-*tert*-butoxycarbonyl-*N*,*N*-bis(4-bromophenyl)amine (1a)

To a solution of *N*,*N*-bis(4-bromophenyl)amine (3 g, 9.3 mmol) and di-*tert*-butyl dicarbonate (3 g, 13.7 mmol) in THF (14 ml), 4-(dimethylamino) pyridine (0.23 g, 1.84 mmol) was added slowly. Then the mixture was heated to reflux overnight with stirring and checked by TLC using ethyl acetate and hexane mixture (1:4) as an eluent. After cooling, the solvent was removed under reduced pressure. The crude product was filtered through a pad of silica gel using dichloromethane as an eluent, concentrated *in vacuo* and then recrystallised from hot methanol to give compound **1a** as a white powder. Yield: 78%. ^1H NMR (400 MHz, $CDCl_3$) δ, ppm: 7.35 (d, J = 8.6 Hz, 4H, Ar), 6.99 (d, J = 8.6 Hz, 4H, Ar), 1.37 (s, 9H, $-CH_3$). ^{13}C NMR (101 MHz, $CDCl_3$) δ, ppm: 153.13, 141.72, 131.95, 128.49, 119.30, 81.98, 28.20. IR (thin film, cm^{-1}): 2980.21, 1708.70, 1487.14, 1311.43, 1285.58, 1252.97, 1152.71, 1071.57, 1050.33, 1009.65, 954.49, 843.36, 819.90, 761.77. MS (ESI) *m/z* for $C_{17}H_{17}Br_2NO_2$, MW = 424.96 (^{79}Br), found 448.01 (^{79}Br, ^{79}Br), 449.99 (^{79}Br, ^{81}Br), 451.91 (^{81}Br, ^{81}Br) $[M+Na]^+$.

N-*tert*-butoxycarbonyl-*N*,*N*-bis[4-(di-(4-methoxyphenyl)amino)phenyl]amine (1b)

Di(4-anisyl)amine (3.56 g, 15.01 mmol), compound **1a** (3g, 7.05 mmol), sodium *tert*-butoxide (2.04 g, 21.22 mmol) and dry toluene (25 mL) were added in a Schlenk flask. The mixture was purged with N_2 for 10 min and then bis(tri-*tert*-butylphosphine)palladium (0) (catalytic amount) was added. The reaction mixture was heated to reflux for 4 h under N_2 atmosphere (TLC control, ethyl acetate and hexane 1:3). After cooling, the reaction was poured into water, extracted with dichloromethane, washed with brine, dried with Na_2SO_4 and concentrated *in vacuo*. The product was purified by column chromatography using ethyl acetate

and hexane (1:3) as an eluent and then recrystallised from hexane to give compound **1b** as a white powder. Yield: 75%. ^{1}H NMR (400 MHz, $CDCl_3$) δ, ppm: 6.94 (dd, *J* = 8.8, 6.5 Hz, 12H, Ar), 6.77 (d, *J* = 8.8 Hz, 4H, Ar), 6.72 (d, *J* = 9.0 Hz, 8H, Ar), 3.70 (s, 12H, -OCH_3), 1.37 (s, 9H, -CH_3). ^{13}C NMR (101 MHz, $CDCl_3$) δ, ppm: 155.73, 154.45, 146.24, 141.05, 135.94, 127.40, 126.37, 120.81, 114.64, 80.71, 55.50, 28.32. IR (thin film, cm^{-1}): 1702.29, 1500.57, 1239.05, 1160.97, 1035.28, 828.40. MS (ESI) *m/z* for $C_{45}H_{45}N_3O_6$, MW = 723.33, found 723.64 $[M]^+$.

_N,N_-bis[4-(di-(4-methoxyphenyl)amino)) phenyl]amine (1c)

Compound **1b** (3.8 g, 5.25 mmol) was dissolved in dichloromethane (20 ml) in a 250 mL three-necked round-bottomed flask. Then trifluoroacetic acid (63 mL, 97 g) was added. The reaction mixture was stirred at room temperature for 10 min (TLC control, ethyl acetate and hexane 1:4). Water was added, the reaction mixture was extracted with toluene and the organic phase was dried with Na_2SO_4. The crude product was concentrated *in vacuo* and recrystallised from toluene and hexane mixture to afford compound **1c** as a green solid. Yield: 82%. ^{1}H NMR (400 MHz, acetone-d_6) δ, ppm: 6.98 (s, 1H, NH), 6.86 (d, *J* = 8.7 Hz, 4H, Ar), 6.80 (d, *J* = 8.7 Hz, 8H, Ar), 6.73 (d, *J* = 8.8 Hz, 4H, Ar), 6.69 (d, *J* = 8.8 Hz, 8H, Ar), 3.61 (s, 12H, -OCH_3). ^{13}C NMR (101 MHz, acetone-d_6) δ, ppm: 155.21, 141.92, 141.47, 124.73, 124.42, 118.18, 114.51, 54.81. IR (thin film, cm^{-1}): 1571.24, 1499.55, 1324.73, 1291.54, 1240.92, 1187.68, 1141.68, 1031.57, 827.34. MS (ESI) *m/z* for $C_{40}H_{37}N_3O_4$, MW = 623.28, found 622.18 $[M-H]^+$.

2,2-Bis(4-metoxyphenyl)acetaldehyde was synthesised by the two-step reaction according to the method described in literature [9].

_N,N_-bis{4-[_N,N_-di(4-methoxyphenyl)] aminophenyl}-_N_-(2,2-diphenylvinyl)amine (HTM-H)

Compound **1c** (0.5 g, 0.62 mmol) was dissolved in THF (10 mL) and diphenylacetaldehyde (DPAA) (0.2 g, 1.02 mmol) was added. The reaction mixture was stirred, heated to reflux for 1 h (monitored by TLC, ethyl acetate and hexane 1:4) and then concentrated *in vacuo*. The crude product was purified by column chromatography using ethyl acetate and hexane (1:5) as an eluent and precipitated from THF and the methanol mixture to afford compound **HTM-H** as a yellow powder. Yield: 22%. ^{1}H NMR (400 MHz, acetone-d_6) δ, ppm: 7.17–6.97 (m, 8H, Ar), 6.84 (d, 2H, Ar), 6.79–6.66 (m, 21H, Ar, =CH-N), 6.55 (d, *J* = 8.5 Hz, 4H, Ar), 3.61 (s, 12H, -OCH_3). ^{13}C NMR (101 MHz, acetone-d_6) δ, ppm: 155.55, 143.93, 141.38, 130.25, 128.05, 127.64, 127.28, 126.17, 125.33, 123.21, 122.85, 114.54, 54.82. IR (thin film, cm^{-1}): 1494.51, 1462.98, 1235.68, 1180.05, 1034.32, 824.88, 722.09, 699.23. MS (ESI) *m/z* for $C_{54}H_{47}N_3O_4$, MW = 801.36, found 801.25 $[M]^+$.

_N,N_-bis{4-[_N,N_-di(4-methoxyphenyl)] aminophenyl}-_N_-[2,2-di(4-methoxyphenyl) vinyl]amine (HTM-OMe)

Compound **1c** (0.5 g, 0.62 mmol) was dissolved in THF (10 mL) and 2,2-bis(4-metoxyphenyl)acetaldehyde (DPAA-OMe) (0.2 g, 0.8 mmol) was added. The reaction mixture was stirred and heated to reflux for 1 h (TLC control, ethyl acetate and hexane 1:4) and then concentrated *in vacuo*. The crude product was purified by column chromatography using ethyl acetate and hexane (1:5) as an eluent and precipitated from THF and the methanol mixture to afford compound **HTM-OMe** as a yellow powder. Yield: 43%. ^{1}H NMR (400 MHz, acetone-d_6) δ, ppm: 7.04 (d, *J* = 8.4 Hz, 2H, Ar), 6.82–6.67 (m, 24H, Ar), 6.58 (t, *J* = 8.2 Hz, 6H, Ar), 6.36 (s, 1H, =CH-N), 3.66 (s, 3H), 3.64 (s, 3H), 3.62 (s, 12H). ^{13}C NMR (101 MHz, acetone-d_6) δ, ppm: 158.80, 158.33, 155.48, 143.59, 141.48, 140.21, 135.13, 131.94, 131.13, 129.30, 128.44, 127.73, 125.22, 122.93, 122.87, 114.53, 113.50, 112.99, 54.80, 54.71, 54.66. IR (thin film, cm^{-1}): 2919.82, 2160.88, 1495.36, 1235.49, 1178.96, 1033.91, 827.09. MS (ESI) *m/z* for $C_{56}H_{51}N_3O_6$, MW = 861.36, found 861.18 $[M^+]$.

RESULTS AND DISCUSSION

Synthesis

Enamines containing 4,4′-dimethoxytriphenylamine units (compounds **HTM-H** and **HTM-OMe**) were synthesised by the multi-step route as shown inScheme 1. In the first step, the secondary amino group of *N,N*-bis(4-bromophenyl)amine was protected with the *tert*-butyloxycarbonyl (BOC) group. In the second step, BOC-protected triamine

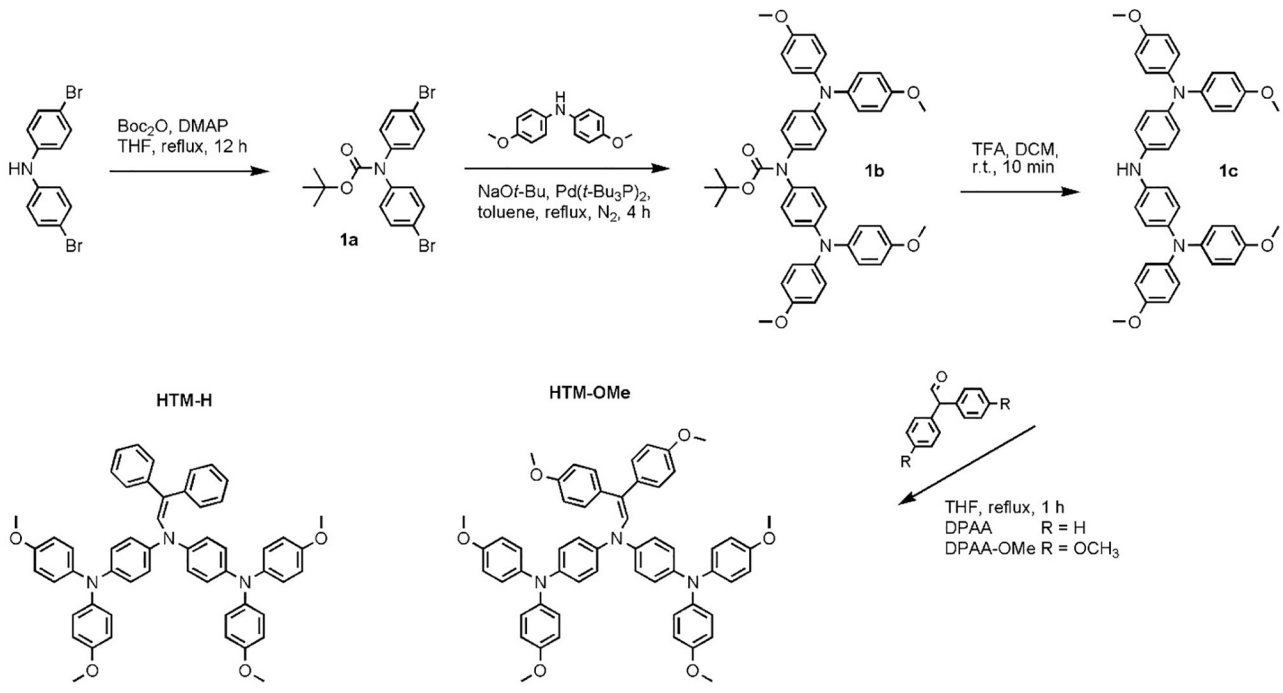

Scheme 1. Synthesis of 4,4′-dimethoxytriphenylamine-based enamines

1b was synthesised from the BOC-protected di(4-bromophenyl)amine **1a** and di(4-anisyl)amine in the presence of bis(tri-*tert*-butylphosphine)palladium (0). In the third step, the BOC group was removed with trifluoroacetic acid (TFA) to yield triamine **1c** [10]. Finally, the treatment of triamine **1c** either with diphenylacetaldehyde (DPAA) or di(4-methoxyphenyl)acetaldehyde (DPAA-OMe) gave enamines **HTM-H** and **HTM-OMe** with the yields reaching 40%.

Thermal properties

Thermal properties of the synthesised compounds were investigated by differential scanning calorimetry (DSC) and thermogravimetric analysis (TGA) under nitrogen atmosphere. The temperatures of the transitions are given in Table 1. The onset temperature of thermal decomposition of the synthesised compounds was attributed to the temperature at 5% weight-loss ($T_{D5\%}$) of the TGA samples. The compounds investigated exhibited a high thermal stability. The $T_{D5\%}$ value for **HTM-H** was established as 425°C while that one for **HTM-OMe** was found to be of 434°C (Fig. 1a). As confirmed by DSC, compounds **HTM-H** and **HTM-OMe** were obtained in an amorphous form after the synthesis and purification. Only glass-to-liquid transitions were observed at 90 and 91°C in both the first and repeated DSC heating scans (Fig. 1b). No crystallisation or melting signals were recorded during either cooling or the repeated heating scans of DSC. Such results indicate a high stability of molecular glasses of compounds **HTM-H** and **HTM-OMe**.

Compounds **HTM-H** and **HTM-OMe** have a similar chemical structure with the difference related to the presence of methoxy groups in the *para*-positions of diphenylethylene fragments. The influence of these additional methoxy groups

Table 1. **Thermal, photophysical and electrooptical characteristics of HTM-H and HTM-OMe**

Compound	$T_{D5\%}$, °C	T_g, °C	λ_{abs}, nm	λ_{PL}, nm	IP_{PE}, eV	λ_{Aon}, nm/E_g^a, eV	EA^b, eV	μ_h^c, cm²/Vs	β^d, (cm/V)$^{1/2}$
	Powder		THF solution/film		film				
HTM-H	425	90	300, 350/306, 352	495/495	5.45	434/2.86	2.55	8.4×10^{-4}	9.7×10^{-3}
HTM-OMe	434	91	300, 350/306, 352	439/476	5.37	429/2.89	2.47	3.6×10^{-4}	6.1×10^{-3}

[a] Calculated using the formula E_g (eV) = 1239.84/λ_{Aon} (nm), where λ_{Aon} is the onset of absorption; [b] calculated using the formula $EA = IP_{PE} - E_g$, [c] taken at ca. 4×10^5 V/cm, [d] obtained by fitting using the formula $\mu_h = \mu_{h0} \exp(\beta \times E^{1/2})$ ($R^2 > 0.98$).

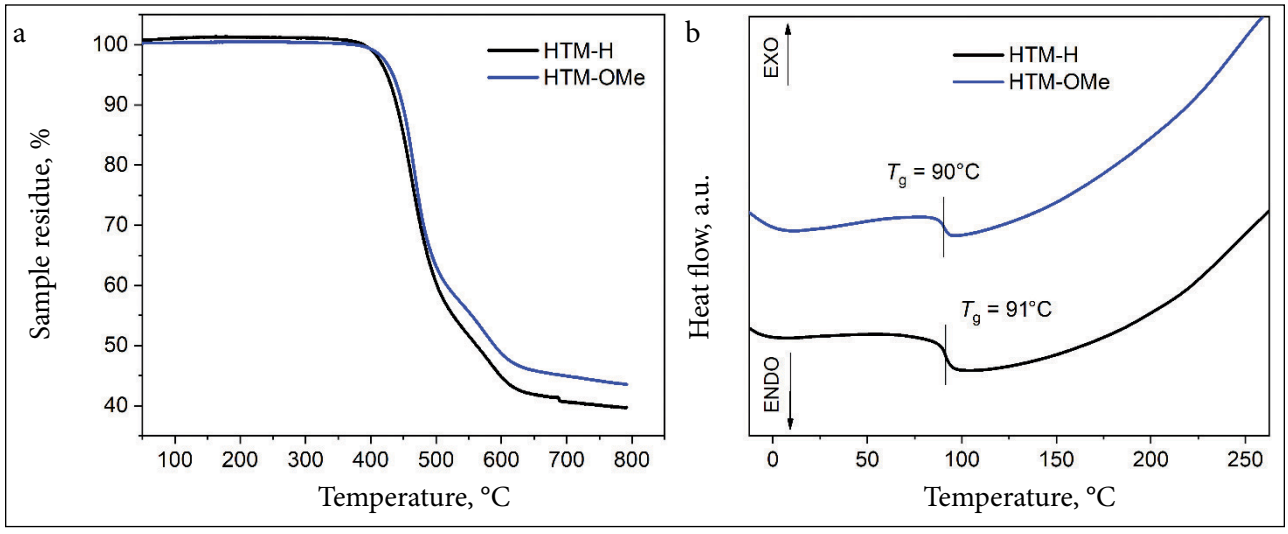

Fig. 1. TGA (a) and DSC curves (b) of compounds **HTM-H** and **HTM-OMe**

on thermal properties can be considered as non-essential. The results of investigation offer valuable insights into the structural influence on thermal characteristics of the synthesised compounds which are crucial for the optimisation of their performance in organic optoelectronic devices such as perovskite solar cells.

Photophysical properties

The UV–Vis absorption and fluorescence spectra of the dilute THF solutions and of the solid films of compounds **HTM-H** and **HTM-OMe** are shown in Fig. 2. The wavelengths of absorption and emission maxima are collected in Table 1. The absorption spectra (Fig. 2a) of both the compounds look nearly the same pointing to a negligible influence of the additional methoxy groups to this property. The attachment of methoxy groups has no influence on the position of absorption peaks. However, it is possible to observe that the long-wave edges (onsets) of the absorption spectra of **HTM-OMe** are blue-shifted by few nanometres compared to those of **HTM-H**.

The absorption spectra of the solutions of both the compounds (solid lines) have two expressed bands with peaks at ca. 300 and 350 nm. The absorption spectra of the corresponding films (dashed lines) look nearly the same. However, they are slightly red-shifted due to intermolecular interactions

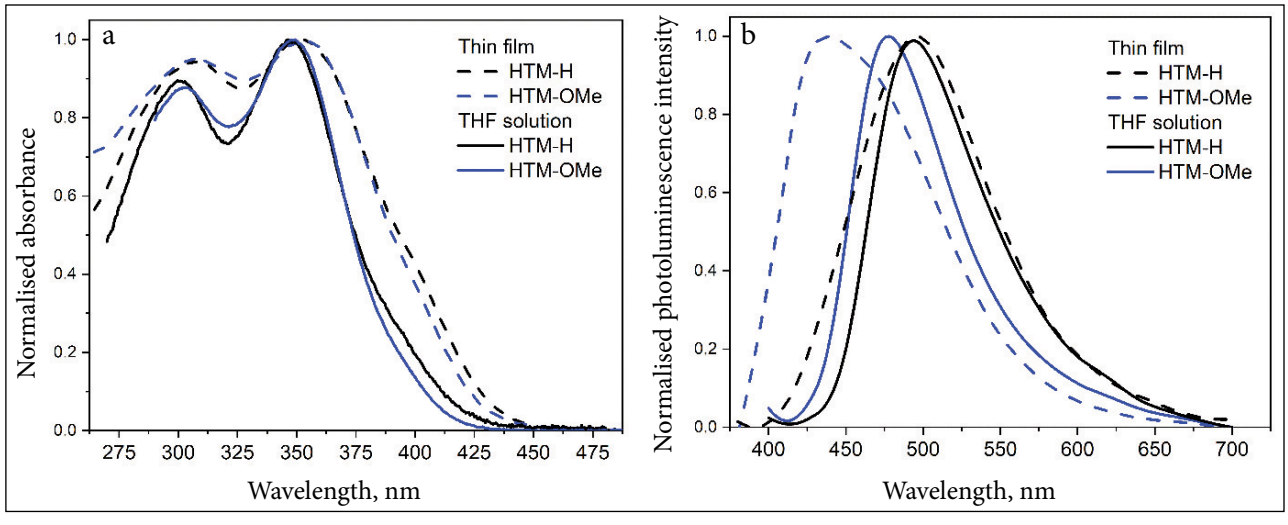

Fig. 2. UV–Vis absorption (a) and fluorescence spectra (b) of the dilute solutions (solid lines) and solid films (dashed lines) of compounds **HTM-H** and **HTM-OMe**

in the solid state. The absorption peak positions of the films are red-shifted by ca. 5 nm compared to those of the solutions. The edges (λ_{Aon}) of absorption were set as ca. 420 nm for the solutions and ca. 430 nm for the films. The optical band-gaps (E_g) estimated from the onset of absorption are situated around 2.9 eV.

More obvious differences might be observed in the fluorescence spectra of compounds **HTM-H** and **HTM-OMe** (Fig. 2b). The fluorescence spectra of the solution and the film of **HTM-H** (black lines) look nearly the same with very close peaks around 495 nm (sky-blue colour). However, the emission band of the film of **HTM-H** (dashed line) is somewhat wider exhibiting the full-width at half-maximum (FWHM) of 104 nm. Meanwhile, FWHM of the emission band of the solution of **HTM-H** solution (solid line) is only of 86 nm. Additionally, the fluorescence band of the film of **HTM-H** is widened mostly to the side of shorter wavelengths. Even more drastic differences are seen between the fluorescence spectra of the solution and film of **HTM-OMe** (blue lines). Firstly, the fluorescence of the film of **HTM-OMe** (dashed line) is obviously blue-shifted with the peak at 438 nm while the corresponding peak of the solution (solid line) is found at 478 nm. The characteristic FWHM values are of 111 nm for the film and of 91 nm for the solution of **HTM-OMe**. The Stokes shifts are set as the energy differences between the peaks of fluorescence band and of the lowest-energy absorption band. These values situate around 1.0 eV except for the film of **HTM-OMe** for which its characteristic Stokes shift is only of 0.7 eV.

Light emission in the solid state of compounds **HTM-H** and **HTM-OMe** occurs from higher energy levels compared to those of the solutions. Apparently, this can be related to restricted molecular motions and thus smaller loss of energy due to rotational and translational ones.

Electrochemical and photoelectrical properties

The energy levels of both the solutions and the solid samples of compounds **HTM-H** and **HTM-OMe** were estimated correspondingly by cyclic voltammetry (CV) and photoelectron emission (EP) spectrometry in air. The data obtained by both the methods are presented in Fig. 3 and Table 1.

The electrochemical properties of the synthesised compounds were investigated using their dichloromethane solutions. The electrochemical oxidation of both the compounds was found to be reversible with half-wave oxidation potential values ($E_{1/2}$) of +0.17 V for **HTM-H** and of +0.13 V for **HTM-OMe** (Fig. 3a). The ionisation energy values (IP_{CV}) were estimated according to $E_{1/2}$ values using the equation $IP_{CV} = 4.8 + E_{1/2vs.FC}$, where $E_{1/2vs.FC}$ is $E_{1/2}$ of the compound investigated *versus* $E_{1/2}$ of ferrocene (Fc). The latest was established to be at 0.0 V. The IP_{CV} values for **HTM-H** and **HTM-OMe** were calculated as 4.97 eV and

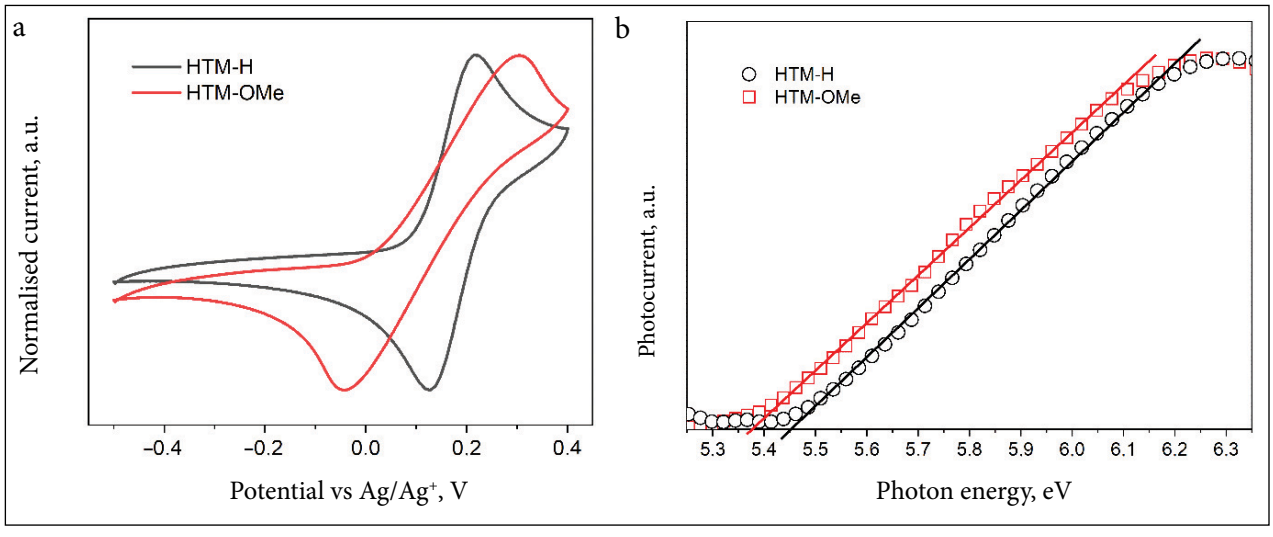

Fig. 3. Cyclic voltammograms of dilute solutions of compounds **HTM-H** and **HTM-OMe** in dichloromethane recorded at a sweep rate of 0.1 V/s at the room temperature (a); photoelectron emission spectra of the solid layers recorded in air (b)

4.93 eV, respectively (Table 1). The electron affinity (EA_{CV}) values calculated using the equation $EA_{CV} = IP_{CV} - E_g$ were found to be located at ca. 2.0 eV.

Solid-state ionisation energies (IP_{PE}) of the HTMs investigated were estimated from their electron photoemission spectra (Fig. 3b). The ionisation potential (the minimum energy required to release an electron from a molecule) was taken as the onset of photocurrent and was calculated through extrapolating the linear incline section of the photocurrent curve. The IP_{PE} values were found to be 5.45 and 5.37 eV, respectively, for compounds **HTM-H** and **HTM-OMe**. Both IP_{CV} and IP_{PE} are slightly lower in the case of **HTM-OMe**. Two additional electron-donating methoxy groups have a small but observable influence on the ionisation potential values of these compounds. A quite big difference of nearly 0.5 eV between IP_{CV} and IP_{PE} can be explained by the different aggregate states of the samples (solution vs solid state).

Charge transporting properties

Charge-transporting properties of compounds **HTM-H** and **HTM-OMe** were studied by the time-of-flight (TOF) method at room temperature. Since both the compounds are of an expressed electron-donating character, current transients with clearly defined transient times (t_{tr}) were recorded for holes only (Fig. 4a–c). No evidence of electron transport was revealed by the TOF measurements.

Hole transport in the thick, vacuum-deposited layers of **HTM-H** and **HTM-OMe** was found to

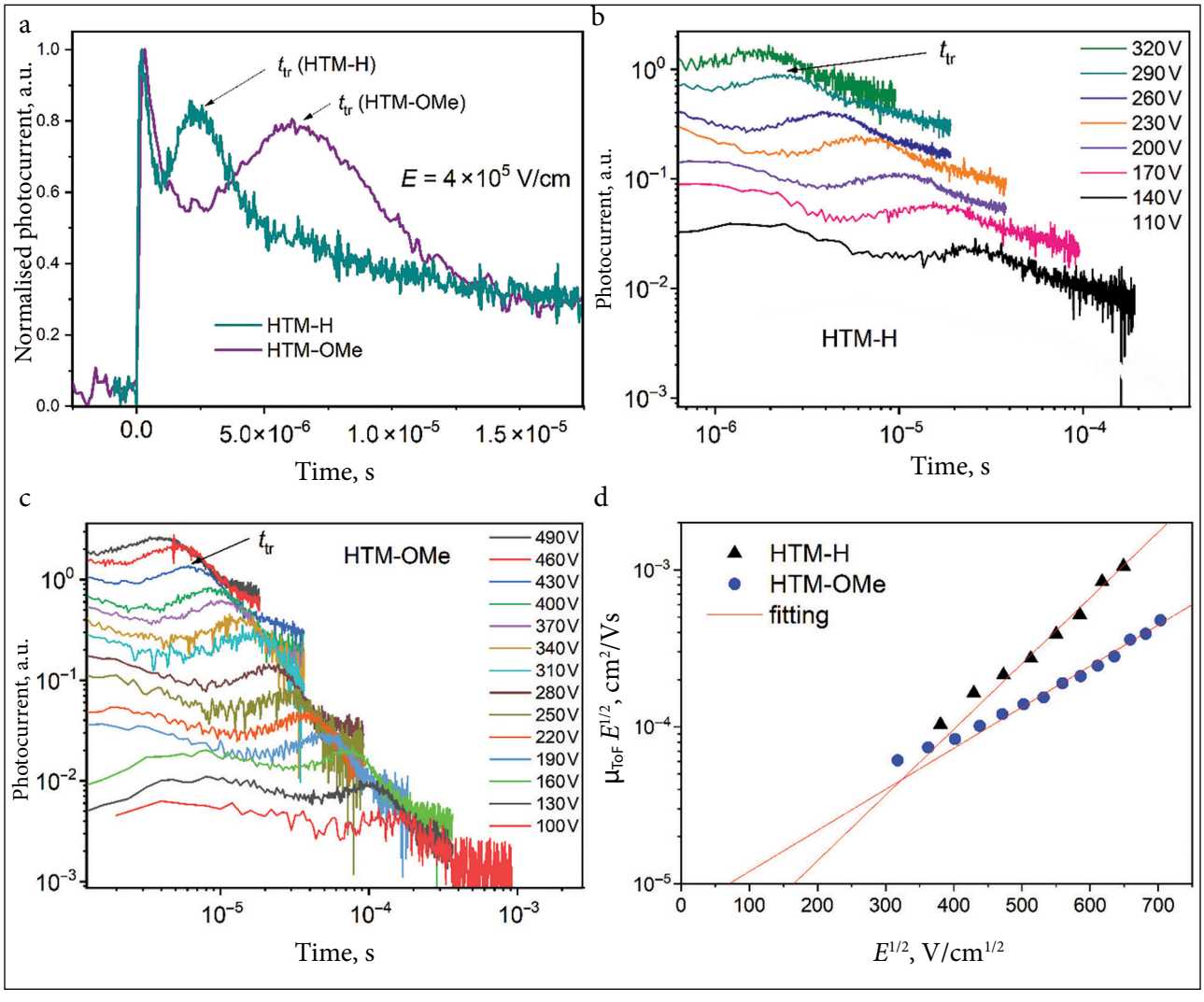

Fig. 4. Transient photocurrents of the samples of **HTM-H** and **HTM-OMe** in the linear scale (a). Transient photocurrents of the samples of **HTM-H** (b) and **HTM-OMe** (c) in the double-logarithmic scale. Electric field dependencies of hole-drift mobilities fitted according to the equation $\mu = \mu_0 \exp(\beta \times E^{1/2})$ (d) for the layers of compounds **HTM-H** and **HTM-OMe** recorded at room temperature

be practically non-dispersive, as t_{tr} values could be obtained even from photocurrent transients built in the linear scale (Fig. 4a). From these photocurrent transients, the t_{tr} value of 2.5 μs was estimated for **HTM-H** and that of 6.3 μs was found to be for **HTM-OMe** at approximately the same electric field (E) of *ca.* 4×10^5 V/cm. As a result, the higher hole mobility (μ_h) of 8.4×10^{-4} cm^2/Vs was found for **HTM-H** compared to 3.6×10^{-4} cm^2/Vs estimated for **HTM-OMe**. Those values were calculated using the equation $\mu_h = d^2/(U \times t_{tr})$, where d is the thickness of a layer and U is the voltage applied to a sample. Such hole mobility values are regarded as high enough for hole-transporting materials used in optoelectronic devices including solar cells and organic light-emitting diodes (OLEDs) [11]. The trend of hole mobility values is similar to that of previously reported for triphenylamine derivatives with methoxy substituents [12]. Taking t_{tr} values from current transients recorded at different voltages (Fig. 4b–c), hole mobilities of **HTM-H** and **HTM-OMe** versus electric field are plotted in Fig. 4d. These hole mobility dependences are in good agreement with the Poole–Frenkel formula $\mu_h = \mu_{h0} \exp(\beta \times E^{1/2})$, where μ_{h0} is the hole mobility at zero electric field, and β is the parameter of electric field dependence. The β values of 9.7×10^{-3} (cm/V)$^{1/2}$ and 6.1×10^{-3} (cm/V)$^{1/2}$ were obtained, respectively, for **HTM-H** and **HTM-OMe** by fitting with a relatively low error ($R^2 > 0.98$). Because of the strong electric field dependence on the hole mobility of **HTM-H**, the μ_h value exceeded 10^{-3} cm^2/Vs at the electric field higher than 4.2×10^5 V/cm (Fig. 4d). On the other hand, the β values of **HTM-H** and **HTM-OMe** are much higher than those of the reported derivatives of triphenylene or enamine [13, 14]. For instance, 1,1-bis(di-4-tolylaminophenyl)cyclohexane showed the β value slightly above 10^{-3} (cm/V)$^{1/2}$ at room temperature [15]. The strong electric-field dependence on the hole mobilities of **HTM-H** and **HTM-OMe** may limit their application in the devices operating under high electric fields, such as OLEDs. This observation can be attributed to the presence of charge carrier traps in the vacuum-deposited films of **HTM-H** and **HTM-OMe** [16]. The molecular structural modifications are necessary to decrease the sensitivity of hole mobilities to electric field.

CONCLUSIONS

We have synthesised and characterised two 4,4′-dimethoxytriphenylamine-based enamines and explored the impact of their structures on the thermal, photophysical, electrochemical and hole-transporting properties. The derivatives form molecular glasses with glass transition temperatures of up to 91°C. Their optical band gaps are of 2.9 eV. Compounds are characterised by comparable ionisation energies (5.37–5.45 eV). Hole mobilities in the thin solid layers of the compounds at the same electric field of 4×10^5 V/cm are of 3.6×10^{-4} cm^2/Vs for the compound with the higher number of methoxy groups and of 8.4×10^{-4} cm^2/Vs for the less methoxylated derivative.

Received 24 February 2026
Accepted 25 February 2026

References

1. S. N. Afraj, A. Velusamy, S. Sharma, et al., *J. Mater. Chem. C*, **13**, 15234 (2025).
2. D. Vaitukaityte, A. Magomedov, K. Rakstys, et al., *RSC Adv.*, **13**, 26933 (2023).
3. M. Steponaitis, M. G. La-Placa, I. C. Kaya, et al., *Energy Fuels*, **4**, 5017 (2020)
4. Z. Li, B.-H. Jo, S.-J. Hwang, et al., *Adv. Sci.*, **6**, 1802163 (2019).
5. Y. Kim, G. Kim, N.-J. Jeon, C. Lim, J. Seo, B.-J. Kim, *ACS Energy Lett.*, **5**, 3304 (2020).
6. J. Keruckas, R. Lygaitis, J. Simokaitiene, J. V. Grazulevicius, V. Jankauskas, G. Sini, *J. Mater. Chem.*, **22**, 3015 (2012).
7. L. Yuan, Q. Xue, F. Wang, et al., *Chem. Rev.*, **125**, 5057 (2025).
8. P. Yan, D. Yang, H. Wang, S. Yang, Z. Ge, *Energy Environ. Sci.*, **15**, 3630 (2022).
9. H. Shi, C. Du, X. Zhang, et al., *J. Org. Chem.*, **83**, 1312 (2018).
10. Y. Hirao, H. Ino, A. Ito, K. Tanaka, T. Kato, *J. Phys. Chem. A*, **110**, 4866 (2006).
11. A. Mondal, L. Paterson, J. Cho, et al., *Chem. Phys. Rev.*, **2**, 031304 (2021)
12. V. Mimaite, J. V. Grazulevicius, R. Laurinaviciute, D. Volyniuk, V. Jankauskas, G. Sini, *J. Mater. Chem. C*, **3**, 11660 (2015).
13. D. Vaitukaityte, Z. Wang, T. Malinauskas, A. Magomedov, G. Bubniene, V. Jankauskas, V. Getautis, H. J. Snaith, *Adv. Mater.*, **30**, 1803735 (2018).
14. P. M. Borsenberger, E. H. Magin, J. J. Fitzgerald, *J. Phys. Chem.*, **97**, 9213 (1993).

15. P. M. Borsenberger, L. Pautmeier, H. Bässler, *J. Chem. Phys.*, **94**, 5447 (1991).
16. H. F. Haneef, A. M. Zeidell, O. D. Jurchescu, *J. Mater. Chem. C*, **8**, 759 (2020).

Jūratė Simokaitienė, Victor Lauroba Manrique, Simas Mačionis, Dmytro Volyniuk, Eigirdas Skuodis, Jonas Keruckas, Juozas V. Gražulevičius

DIMETOKSITRIFENILAMINO FRAGMENTUS TURINČIŲ ENAMINŲ SINTEZĖ IR SAVYBĖS

S a n t r a u k a

Šiame straipsnyje aprašoma naujų trifenilamino fragmentus turinčių enaminų sintezė ir savybės. Ištirtos šių junginių terminės, fotofizikinės bei elektrocheminės charakteristikos. Fotoelektronų emisijos spektroskopijos metodu nustatytos šių junginių jonizacijos energijos. Lėkio trukmės metodu ištirtos enaminų sluoksnių skylių pernašos savybės. Nustatyta, kad junginiai sudaro molekulinius stiklus, kurių stiklėjimo temperatūra siekia 91 °C. Junginiams būdinga 2,9 eV pločio draudžiamoji juosta ir panašios jonizacijos energijos (5,37–5,45 eV). Skylių judris junginių plonuose kietuose sluoksniuose, esant $4{,}2 \times 10^5$ V/cm stiprio elektriniam laukui, siekia $8{,}4 \times 10^{-4}$ cm^2/Vs.